

# Synthesis and characterization of Nano NiCo<sub>2</sub>O<sub>4</sub> by microwave promoted precipitation method

M Yang, A Chen, Y Zhang and L Le

School of Environment and Chemical Engineering, Dalian Jiaotong University, Dalian 116028, China

Email: minyang@djtu.edu.cn

**Abstract.** Nanostructured spinel NiCo<sub>2</sub>O<sub>4</sub> was synthesized via a facile and effective microwave promoted precipitation method with a simple post-calcination treatment. The crystalline and textural structure and morphology of the samples were characterized by X-ray diffraction, field-emission scanning electron microscopy, and Brunauer-Emmett-Teller techniques. The influence of several parameters on the morphology of NiCo<sub>2</sub>O<sub>4</sub>, such as Ni/Co mole ratio, amount of precipitation agent urea, amount of ethylene glycol (EG), were investigated, and the optimal reaction conditions (Ni/Co = 1.0:2.5, urea 0.30 g, and EG 30 ml) were obtained. Under the optimal reaction conditions, the prepared spinel NiCo<sub>2</sub>O<sub>4</sub> has a regular porous nanosheet structure. The nanosheet spinel NiCo<sub>2</sub>O<sub>4</sub> possesses a high surface area of 124.8 m<sup>2</sup>/g, a narrow pore size distribution of 3–10 nm, and a mean pore diameter of 5.4 nm.

## 1. Introduction

Electrochemical energy storage device will become more and more important in the future societies because of the ever-increasing energy consumption and the limited supply of fossil fuels combined with the urgent need to reduce CO<sub>2</sub> emissions [1, 2]. Because the supercapacitors, one kind of the currently available electrochemical energy storage device, can supply a high-power/energy density, long lifespan, fast charge and discharge process, and excellent reversibility, they have attracted much significant attention in the entire world [3-5]. The performance of the supercapacitors significantly depends on the applied electrode materials [6], and this electrochemical energy-storage technology has been intensely impacted by nanoscience and technology [7].

Nanostructured materials are attractive as electrode materials because of their large specific surface area and the smaller size. A larger surface area of electrode materials can provide numerous electroactive sites and can efficiently accommodate the mechanical strain caused by volume variation during the cycling process, promoting the capacities through the surface storage mechanism. The smaller size of electrode materials can also shorten the ion- and electron-transport pathways and enhance phase transformation. Among all the materials used for electrode material, nanostructured transition-metal oxides are proved to be one type of promising material for applications in energy-related systems. Therefore, nanostructured transition-metal oxides are widely investigated, and the related study has resulted in increased electrochemical performance for supercapacitors [8, 9]. Among the different nanostructured mixed-metal oxides, the spinel NiCo<sub>2</sub>O<sub>4</sub>, a binary oxide, has been considered as the most promising alternative material because it possesses many advantages such as low cost, abundant resource, environmental friendliness, and so on [10,11]. More attractively, the spinel NiCo<sub>2</sub>O<sub>4</sub> can offer higher electrochemical activity and better electrical conductivity than the two single component oxides, nickel oxide and cobalt oxide [12]. Because of the special feature compared



to other nanostructured transition-metal oxides materials,  $\text{NiCo}_2\text{O}_4$  has been widely investigated as the high-performance electrode material for supercapacitors [11, 13]. Various synthesis techniques, such as co-precipitation, sol-gel, solid state reaction, and hard template method, have been employed to prepare nanostructured  $\text{NiCo}_2\text{O}_4$  with different shapes and sizes. With surfactant assistance, Shen et al.[14] reported a simple hydrothermal method with subsequent annealing treatment to grow mesoporous  $\text{NiCo}_2\text{O}_4$  nanowire arrays on carbon textiles with strong adhesion. Using a general solution method combined with a subsequent simple heat treatment, Zhang and Lou have prepared the interconnected mesoporous  $\text{NiCo}_2\text{O}_4$  nanosheets which were grown on different conductive substrates [15].

Even if there are many different synthesis techniques to prepare the spinel  $\text{NiCo}_2\text{O}_4$ , the microwave method has become one of the most attractive techniques owing to its intrinsic advantages, including short heating time and homogeneous thermal transmission [16, 17]. The efficient energy transfer of the microwave can result in a rapid heating process. Furthermore, the homogeneous heating of the precursor solution caused by microwave heating can result in a rather short time to obtain a uniform distribution of particle size. Consequently, the microwave hydrothermal process is more efficient than the conventional hydrothermal process for preparing various oxide nanoparticles. In this paper, we report the synthesis of mesoporous  $\text{NiCo}_2\text{O}_4$  nanomaterials through a facile microwave method followed by calcination in air..

## 2. Experiments

### 2.1. Synthesis of $\text{NiCo}_2\text{O}_4$

In the  $\text{NiCo}_2\text{O}_4$  synthesis process, a certain amount of  $\text{Ni}(\text{NO}_3)_2 \cdot 6\text{H}_2\text{O}$  and  $\text{Co}(\text{NO}_3)_2 \cdot 6\text{H}_2\text{O}$  were dissolved in deionized (DI) water to form a homogeneous solution. Urea and ethylene glycol (EG) were added into the above solution and stirred for 2 h. The formed solution was heated to  $140\text{ }^\circ\text{C}$  and heating for 30 min in a microwave synthesizer, and, then, the mixed solution was cooled to room temperature. When the solution became clear, the green precipitate was filtered, and washed with DI water and ethanol several times alternatively. The obtained precipitate was dried at  $80\text{ }^\circ\text{C}$  in an oven for 12 h. After that, the dried material was transferred to a muffle oven and the temperature was increased to  $300\text{ }^\circ\text{C}$  with a heating rate of  $1\text{ }^\circ\text{C}/\text{min}$  and kept at  $300\text{ }^\circ\text{C}$  for 3 h to obtain nanometer  $\text{NiCo}_2\text{O}_4$  samples.

### 2.2. Characterization

The crystallographic information of the synthesized  $\text{NiCo}_2\text{O}_4$  nanomaterials were studied by using an Empyrean X-Ray diffractometer (Panalytical, Holland) using nickel-filtered  $\text{Cu K}\alpha$  radiation ( $\lambda=0.15405\text{ nm}$ ) at 40 kV and 30 mA. Field emission scanning electron microscopy (FE-SEM) was recorded digitally on a Zeiss Supra55 (VP) (Zeiss, Germany) with an EDX attachment microscope operating at 30 kV to examine the morphology and structure of the material. The specific surface area and the porosity distributions were calculated by using BET nitrogen adsorption/desorption isotherms and the Barrett-Joyner-Halenda (BJH) method, respectively, by using a Micromeritics ASAP 2000 surface characterization analyzer using  $\text{N}_2$  adsorption at 77K.

## 3. Results and Discussion

### 3.1. Influence of Reaction Conditions on Morphology of nano $\text{NiCo}_2\text{O}_4$

**3.1.1. Influence of Ni/Co ratio.** The morphology of the  $\text{NiCo}_2\text{O}_4$  nanomaterials synthesized under different Ni/Co mole ratio observed by field-emission scanning electron microscopy is illustrated in Figure1. The FE-SEM results in Fig.1 show that when the ratio of Ni/Co was 1.0:2.0, the morphology of  $\text{NiCo}_2\text{O}_4$  sample was heterogeneous. There are some microchips with irregular shape and some polygon formed by microchips with obvious agglomeration. When the ratio of Ni/Co was 1.0:2.5, the  $\text{NiCo}_2\text{O}_4$  sample shows nanosheet structure with regular shape and size. At the same time, the agglomeration was well improved, leading to the sample having homogeneous morphology. The

surface of the sample is very clear, indicating that the sample has high purity. When the ratio of Ni/Co was up to 1.0:3.0, the sample has relatively regular morphology, but it is difficult to recognize the single nanosheet. In fact, the nanosheets in the sample tend to agglomerate, along with its shape turning from nanosheet to the mixture of nanosheet and rod. But at the same time, the density of particles in this sample was very high; therefore, the collision between the particles leads to the growth of the particles, as well as increasing of the agglomeration phenomenon. Considering the morphology and structure of  $\text{NiCo}_2\text{O}_4$ , the suitable ratio of Ni/Co is 1.0:2.5.

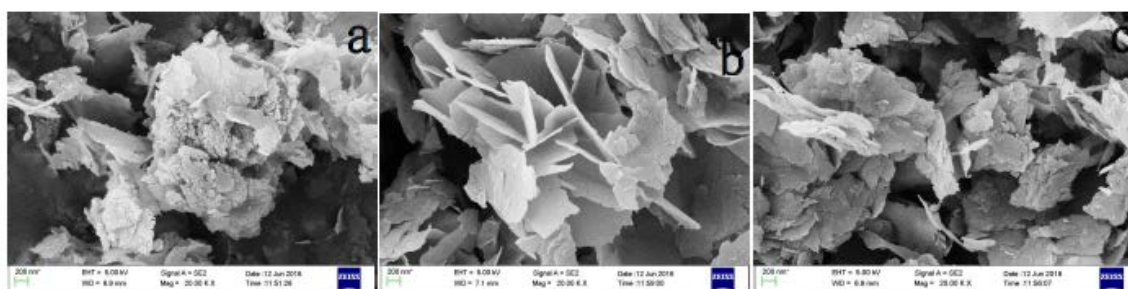


**Figure 1.** FE-SEM images of nano  $\text{NiCo}_2\text{O}_4$  prepared under different Ni/Co ratio (a) Ni/Co = 1.0:2.0 (b) Ni/Co = 1.0:2.5 (c) Ni/Co = 1.0:3.0 (Reaction conditions:  $\text{Ni}(\text{NO}_3)_2 \cdot 6\text{H}_2\text{O}$  1 mmol; urea 5 mmol; EG 45 ml).

**3.1.2. Influence of urea amount.** Figure 2 shows the FE-SEM images of the  $\text{NiCo}_2\text{O}_4$  samples prepared under different urea amount. While amount of urea participating in reaction nearly didn't affect the crystal structure of  $\text{NiCo}_2\text{O}_4$ , it has influence on particles' morphology. Fig.2 shows when the amount of urea was 0.24 g (the molar ratio of  $\text{Ni}(\text{NO}_3)_2 \cdot 6\text{H}_2\text{O}$  and urea was 1:4), there are lots of small particles between the big ones, which indicated the formation of Ni-Co based precursor was incomplete. As the amount of urea increases to 3.0 g, i.e. molar ratio of  $\text{Ni}(\text{NO}_3)_2 \cdot 6\text{H}_2\text{O}$  and urea was 1:5, the particles of  $\text{NiCo}_2\text{O}_4$  presented more regular morphology, and became uniform. All the particles were well dispersed and the nanosheet structure can be recognized. However, when the amount of urea reached to a higher extent 0.36 g (molar ratio of  $\text{Ni}(\text{NO}_3)_2 \cdot 6\text{H}_2\text{O}$  and urea being 1:6), agglomeration tends to happen. This may be due to the reason that excessive urea accelerates hydrolysis process, thus negatively influencing the formation of Ni-Co based precursor. Hence, it can be drawn that suitable amount of urea was 3.0 g, herein, the molar ratio of  $\text{Ni}(\text{NO}_3)_2 \cdot 6\text{H}_2\text{O}$  and urea was 1:5.

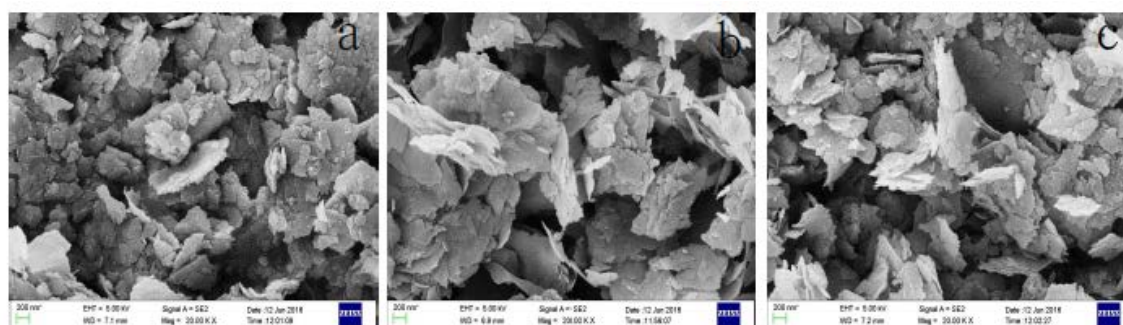


**Figure 2.** FE-SEM images of nano  $\text{NiCo}_2\text{O}_4$  prepared using different urea amount (a) urea 0.24 g (b) urea 0.30 g (c) urea 0.36 g (Reaction conditions: Ni/Co = 1.0:2.5; EG 45 ml).

**3.1.3. Influence of EG amount.** During the synthesis process of  $\text{NiCo}_2\text{O}_4$ , the Ni-Co based precursor was formed through the well-known hydrolysis and precipitation process. As one step-by-step released pH adjusting precipitation agent, urea can generate  $\text{OH}^-$  ions slowly under reaction condition. In the

reaction system, the formed OH<sup>-</sup> ions can react with Ni<sup>2+</sup> and Co<sup>2+</sup> to form Ni-Co based precursor. The crystal growth of Ni-Co based precursor can be affected by the formation rate of OH<sup>-</sup> ions, i.e. the hydrolysis rate of urea. At the same time, the ethylene glycol (EG) can assist the crystal growth of Ni-Co based precursor to form nanosheet structure materials. After calcination, the nanosheet NiCo<sub>2</sub>O<sub>4</sub> can be obtained from the Ni-Co based precursor. This means that the EG should influence the formation of NiCo<sub>2</sub>O<sub>4</sub> nanomaterials. So, the amount of ethylene glycol was changed to study its effect on the NiCo<sub>2</sub>O<sub>4</sub> synthesis, and the FE-SEM images of the NiCo<sub>2</sub>O<sub>4</sub> nanoparticles prepared with different EG amount were presented in Figure 3.

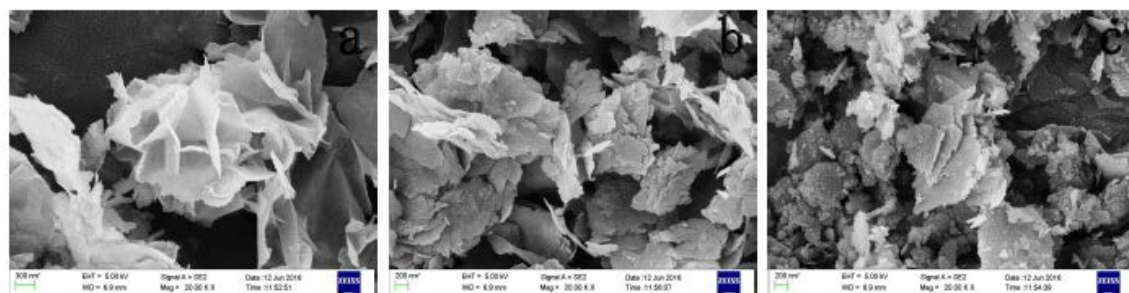


**Figure 3.** FE-SEM images of nano NiCo<sub>2</sub>O<sub>4</sub> prepared under different EG amount (a) EG 30 ml (b) EG 45 ml (c) EG 60 ml (Reaction conditions: Ni/Co = 1.0:2.5; urea 0.30 g ).

It can be seen from Figure 3 that the amount of EG has a big affect on the morphology of NiCo<sub>2</sub>O<sub>4</sub> nanomaterials. When the amount of EG was 30 ml, the NiCo<sub>2</sub>O<sub>4</sub> nanoparticles possess a very thin and regular nanosheet structure and the nanosheets are interconnected with each other with a rippled-silk morphology. When the amount of EG was increased to 45 ml, the particles of the NiCo<sub>2</sub>O<sub>4</sub> agglomerated to formed in thick nanosheet, and the nanosheets had a relatively smaller size than that when the amount of EG being 30 ml. When the amount of EG reached to 60 ml, product size became uneven. Furthermore, viewed from image, particle agglomeration became very severe, resulting in that the NiCo<sub>2</sub>O<sub>4</sub> nanomaterials did not show nanosheet structure. Thus, the amount of EG of 30 ml seems to be the most favorable.

The above results show that the optimal reaction conditions for NiCo<sub>2</sub>O<sub>4</sub> nanomaterials are Ni/Co = 1.0:2.5 (Ni(NO<sub>3</sub>)<sub>2</sub>·6H<sub>2</sub>O 1 mmol), urea 0.30 g (5 mmol), and EG 30 ml. NiCo<sub>2</sub>O<sub>4</sub> nanomaterials prepared under the conditions possess a nanosheet structure, and present wrinkled silk-like thin sheets, which implies that the sample should have a high surface area. These nanosheets in NiCo<sub>2</sub>O<sub>4</sub> nanomaterial contain numerous mesopores with abundant open space and electroactive sites (Figure 3 a). The surface composition of NiCo<sub>2</sub>O<sub>4</sub> materials were determined by EDX attachment of Zeiss Supra55 (VP). The EDX results show that there were Ni, Co, and O atoms existing on the surface of the prepared sample. In order to obtain more information about the crystalline structure and textural structure of the prepared NiCo<sub>2</sub>O<sub>4</sub> nanosheets, XRD and BET techniques were performed and the results are discussed.

### 3.2. XRD Results

The crystallographic phase purity of the samples synthesized under the optimal reaction conditions is examined by X-ray diffraction (XRD). The XRD pattern (Figure 4) reveals the phase purity and crystalline structure of the prepared NiCo<sub>2</sub>O<sub>4</sub> nanosheets. The peaks appearing at 2θ of 18.9°, 31.3°, 36.7°, 44.4°, 59.1°, 64.9° can be easily indexed as (111), (220), (311), (400), (511), and (440) crystalline planes, and are in good agreement with the spinel NiCo<sub>2</sub>O<sub>4</sub> crystalline structure (JCPDS card no. 20-0781). No impurity peaks were identified. All the corresponding peaks have widen feature, indicating that the sample may has mesoporous structure.

### 3.3. BET Results

To obtain more detailed information about structure of the as-prepared  $\text{NiCo}_2\text{O}_4$ , the Brunauer Emmett Teller (BET) measurements are performed and the corresponding results presented in Figure 5. The  $\text{N}_2$  adsorption/desorption isotherm of the sample shows the typical hysteresis loop in the relative pressure range of 0.6–1.0  $P/P_0$ , which suggesting the presence of mesoporous structure [18]. This is in accordance with the results in XRD mentioned above. The nitrogen adsorption–desorption isotherm shown in Figure 5 is a type-IV isotherm, as defined by the IUPAC, with a sharp step at intermediate relative pressures. The isotherm, shows two well-defined stages can be identified, (a) a slow increase in nitrogen uptake at 0.0–0.6 relative pressures, corresponding to monolayer–multilayer adsorption on the pore walls, (b) a sharp step at 0.6–0.95 relative pressures indicative of capillary condensation in mesopores.

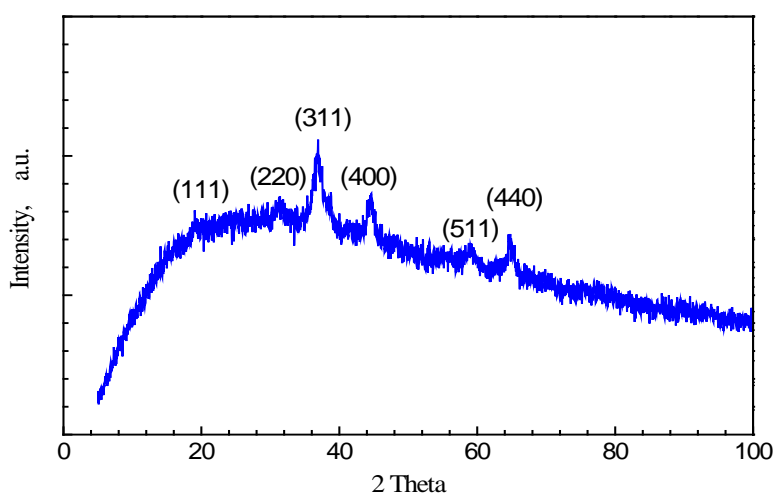


**Figure 4.** XRD pattern of nano  $\text{NiCo}_2\text{O}_4$  synthesized under the optimal reaction conditions. The mesoporous  $\text{NiCo}_2\text{O}_4$  nanosheet shows a high Brunauer–Emmett–Teller (BET) specific surface area of  $129 \text{ m}^2/\text{g}$  with a narrow BJH adsorption pore size distribution of 3–10 nm (Figure 5, inset), a pore volume of  $0.43 \text{ cm}^3/\text{g}$ , and a hydraulic mean pore diameter ( $d_h = 4V_p/S_{\text{BET}}$ ) of 5.4 nm.

## 4. Conclusions

In summary, spinel  $\text{NiCo}_2\text{O}_4$  nanomaterials have been successfully synthesized via a facile and effective microwave promoted precipitation method followed by calcination treatment. From the obtained results we find that the Ni/Co mole ratio, amount of precipitation agent urea, and amount of ethylene glycol have significant influence on the morphology of the samples. Under the optimal reaction conditions (Ni/Co = 1.0:2.5, urea 0.30 g, and EG 30 ml), the prepared  $\text{NiCo}_2\text{O}_4$  nanomaterials have pure spinel crystalline and a regular mesoporous nanosheet structure. The spinel  $\text{NiCo}_2\text{O}_4$  nanosheet possesses a high surface area of  $124.8 \text{ m}^2/\text{g}$ , a narrow pore size distribution of 3–10 nm, and a mean pore diameter of 5.4 nm.

## Acknowledgments

Authors wishing to acknowledge supports from the Science and Technology Innovation Fund for College Student of Dalian Jiaotong University and the Project of Liao Ning the University Students' Innovation are greatly appreciated.

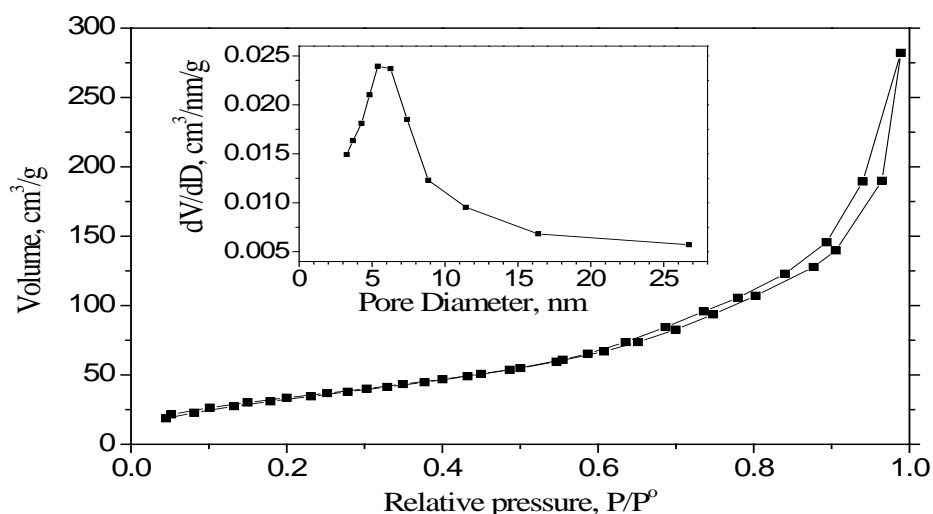


**Figure 5.** N<sub>2</sub> adsorption/desorption isotherm and the corresponding BJH pore size distributions (inset) of nano NiCo<sub>2</sub>O<sub>4</sub> synthesized under the optimal reaction conditions.

## References

- [1] Mai L, Tian X, Xu X, Chang L and Xu L 2014 *Chem. Rev.* 114 11828–62
- [2] Zhang G, Wang T, Yu X, Zhang H, Duan H, Lu B 2013 *Nano Energy* 2 586–94
- [3] Lu Q, Chen J, and Xiao J 2013 *Chem. Int. Ed.* 52 1882–9
- [4] Wang X, Yan C, Sumboja A, Lee P S 2014 *Nano Energy* 3 119–26
- [5] Simon P and Gogotsi Y 2008 *Nat. Mater.* 7 845–54
- [6] Simon P and Gogotsi Y 2013 *Acc. Chem. Res.* 46 1094–103
- [7] Zhao X, Sanchez B M, Dobson P J and Grant P S 2011 *Nanoscale*, 3 839–55
- [8] Banerjee A, Aravindan V, Bhatnagar S, Mhamane D, Madhavi S, Ogale S 2013 *Nano Energy* 2 890–6
- [9] Wang X, Li X, Sun X, Li F, Liu Q, Wang Q and He D 2011 *J. Mater. Chem.* 21 3571–3
- [10] Gao G, Wu H B, Ding S, Liu L M and Wen X 2015 *Small* 11 804–8
- [11] Zhou Q, Xing J, Gao Y, Lv X, He Y, Guo Z, and Li Y 2014 *ACS Appl. Mater. Interfaces* 6 11394–402
- [12] Li L, Peng S, Cheah Y, Teh P, Wang J, Wee G, Ko Y, Wong C and Srinivasan M 2013 *Chem. Eur. J.* 19 5892–8
- [13] Li J, Xiong S, Liu Y, Ju Z and Qian Y 2013 *ACS Appl. Mater. Interfaces* 5 981–8
- [14] Shen L, Che Q, Li H and Zhang X 2014 *Adv. Funct. Mater.* 24 2630–7
- [15] Zhang G and Lou X W 2013 *Adv. Mater.* 25 976–9
- [16] Krishnakumar T, Jayaprakash R, Parthibavarman M, Phani A R, Singh V N and Mehta B R 2009 *Mater. Lett.* 63 896–8
- [17] Yang M, Wang J, C Xiao and H Zhao 2016 *Integrated Ferro.* 172 1–9
- [18] Vinu A, Sawant D P, Ariga K, Hartmann M and Halligudi S B 2005 *Microporous Mesoporous Mater.* 80 195–203